Increasing Antibacterial Efficiency of Cu Surfaces by targeted Surface Functionalization via Ultrashort Pulsed Direct Laser Interference Patterning

Daniel W. Müller,* Sarah Lößlein, Emmanuel Terriac, Kristina Brix, Katharina Siems, Ralf Moeller, Ralf Kautenburger, and Frank Mücklich

Copper (Cu) exhibits great potential for application in the design of antimicrobial contact surfaces aiming to reduce pathogenic contamination in public areas as well as clinically critical environments. However, current application perspectives rely purely on the toxic effect of emitted Cu ions, without considering influences on the interaction of pathogenic microorganisms with the surface to enhance antimicrobial efficiency. In this study, it is investigated on how antibacterial properties of Cu surfaces against *Escherichia coli* can be increased by tailored functionalization of the substrate surface by means of ultrashort pulsed direct laser interference patterning (USP-DLIP). Surface patterns in the scale range of single bacteria cells are fabricated to purposefully increase bacteria/surface contact area, while parallel modification of the surface chemistry allows to involve the aspect of surface wettability into bacterial attachment and the resulting antibacterial effectivity. The results exhibit a delicate interplay between bacterial adhesion and the expression of antibacterial properties, where a reduction of bacterial cell viability of up to 15-fold can be achieved for *E. coli* on USP-DLIP surfaces in comparison to smooth Cu surfaces. Thereby, it can be shown how the antimicrobial properties of copper surfaces can be additionally enhanced by targeted surface functionalization.

1. Introduction

The decreasing effectiveness of antibiotics in fighting infectious diseases is a growing problem not only in hospitals and public spaces, but even on the International Space Station, where biofilms might also induce hazardous system failure by biofouling.[1] Current estimates by the World Health Organization (WHO) suggest that the number of deaths caused by multidrug-resistant bacteria worldwide could rise to ten million per year by 2050, if the current trend continues.[2] One way to fight both critical biofilm formation as well as the spreading of infectious diseases is to reduce the survivability of bacteria on technically and frequently touched contact surfaces, by using actively antimicrobial materials like copper (Cu) and silver (Ag) that are not based on pharmaceutical antibiotics. Here, Cu shows great potential for a wider application,[3,4] looking back to a multi-millennial history of repeated rediscovery of its aseptic properties,[5] while it is also involved as a trace element in central processes of human metabolism.[6] In contrast, Ag exhibits toxicity at low quantities,[7] by which dosing has to be precisely adjusted in case of antimicrobial application to avoid a negative immune response.[8] Due to the toxic effect of released Cu ions, bacteria[9,10] as well as viruses[11] are rapidly killed in both dry and moist environments, when adhering to Cu surfaces. The antimicrobial properties of Cu are closely linked to both the amount of ions released and absorbed by the attacked microorganism, whereby specific effects have to be considered when using Cu as an antimicrobial agent: 1) It

D. W. Müller, S. Lößlein, Prof. F. Mücklich
Chair of Functional Materials
Department of Materials Science
Saarland University
Saarbrücken 66123, Germany
E-mail: daniel.mueller@uni-saarland.de

The ORCID identification number(s) for the author(s) of this article can be found under https://doi.org/10.1002/admi.202001656.

Dr. E. Terriac
Leibniz Institute for New Materials
Dynamic Biomaterials
Saarbrücken 66123, Germany
Dr. K. Brix, Dr. R. Kautenburger
Department of Inorganic Solid-State Chemistry
Elemental Analysis
Saarland University
Saarbrücken 66123, Germany
K. Siems, Prof. R. Moeller
Aerospace Microbiology
Radiation Biology Department
Institute of Aerospace Medicine
German Aerospace Center (DLR e.V.)
Cologne 51147, Germany

ADVANCED
SCIENCE NEWS
www.advancedsciencenews.com

ADVANCED
MATERIALS
INTERFACES
www.advmatinterfaces.de

has been shown that close contact to the Cu surface is mandatory to achieve a high antimicrobial effectiveness.[12] Since bacteria act as reservoirs for released Cu ions, close contact to the surface might reduce the self-passivation of the copper surfaces through oxide formation, whereby the ion release can be kept constantly high.[13] 2) Cu surfaces might face reduced antimicrobial efficiency in certain cases of corrosion/aging, as its stabilizing oxides CuO and Cu_2O show either less, or similar antimicrobial efficiency as the pure metal, respectively.[14] 3) Bacteria have to be exposed for sometimes up to 3 h to the Cu surface to achieve a sufficient reduction of 99.9% of viable cell count.[11,13] Against this background, it is essential to understand how the antimicrobial capacity of copper-based materials can be both increased and maintained to allow for an efficient adaptation of its functional properties for different kinds of antimicrobial application.

Attempts to enhance the antibacterial properties and especially the speed of bacterial reduction of Cu mainly focused on its application as nanoparticles distributed in liquid or solid matter for several years, similar to Ag.[8,15–20] However, recent results suggest a negligible antibacterial impact of the low particle sizes, as bacterial killing by Cu nanoparticles was actually shown to be mainly linked to Cu ion release rate instead of absorption of the nanoparticles.[21] Another promising approach involves the functionalization of the Cu substrate surfaces, as it has been shown that bacteria respond quite sensitively to chemical and topographic surface properties, where especially wettability and features in the micro- and nanometer range appear to exhibit the highest effect: Using bacterial probe atomic force microscopy, Maikranz et al.[22] were recently able to determine a significantly enhanced adhesion force of *Staphylococcus aureus* on Si substrates, which were chemically modified to exhibit hydrophobic wetting behavior, compared to unmodified hydrophilic Si. Similar behavior was observed in previous studies, where different bacterial strains showed higher adhesion on hydrophobic polymer surfaces compared to hydrophilic glass and metal surfaces.[23,24] In contrast, Lutey et al.[25] detected a stronger reduction of bacterial retention on hydrophobic compared to hydrophilic steel surfaces, where both were treated by ultrashort laser pulses to form laser-induced periodic surface structures (LIPSS). In this context, they claimed that surface topography actually plays a more significant role on bacterial adhesion than wetting properties, as a parallel sample group exhibiting higher topographic feature size showed even increased adhesion in case of *Escherichia coli*.[25] The actual relation between topographic roughness/structuring to bacterial size was indeed proven to play a major role in bacterial adhesion in various studies, where topographic features matching the size of the tested bacteria enhance attachment, while lower feature sizes reduce it, which lead to sometimes contrary effectivity of a specific surface topography against different bacterial strains.[26–31]

Following the approach of topographically induced antimicrobial surface properties further on, a number of natural blueprints like the *Cicada* and *Dragonfly* wings are available where prevention of adhesion alters into mechanically triggered killing of bacteria by piercing and structurally damaging the bacterial cell wall when micro- and nanometer-scaled surface structures exhibit high aspect ratios.[32,33] This functional approach was

successfully applied many times, so far, also involving more technically oriented surfaces like, for example, black silicon[34] and oxidic nanostructures on Ti surfaces.[35,36] However, the bactericidal interaction of these types of surfaces is tightly connected to chemically induced attractive forces between bacteria and surface to enable mechanical damage of the cell walls.[32] It was also proven that particular structure types are highly effective for certain bacterial strains, while others may not be affected to a similar extent.[37]

First approaches involving functional surface properties on antimicrobial copper surfaces highlighted the possibility to reduce bacterial transmission by hydrophobic wetting similar to the lotus effect.[18,19] In more recent studies, both Boinovich et al.[38] and Selvamani et al.[39] achieved antibacterial efficiency exceeding the copper-based reference material by the coupled effect of surface roughening and enhanced wettability induced by short pulsed laser treatment. Here, soaking of the deposited liquid into the porous surface structure forces the bacteria against the hierarchically scaled surface features resulting in structural cell membrane damage,[38–40] similar to the killing mechanism of bacteria piercing surface topographies on *Cicada* or *Dragonfly* wings.[32,33] Unfortunately, antibacterial efficiency decreases strongly as soon as the surfaces stabilize at hydrophobic wetting,[38,41] which is most likely linked to the dense superficial layer of CuO initiated during short pulsed laser processing[42] showing reduced antimicrobial capacities due to reduced Cu ion release.[14] Therefore, it is important to include all functional aspects of their antiseptic effectiveness when specifically optimizing antimicrobial copper surfaces in order to maintain the positive effects over a longer period of time.

As former research has proven the impact of functional surface properties on the bacteria/surface interaction,[25,28] a suitable modification of the surface properties might positively affect the antibacterial efficiency of copper surfaces. Here, we introduce a novel methodology to enhance antimicrobial properties of Cu surfaces by topographic as well as chemical modification using ultrashort pulsed direct laser interference patterning (USP-DLIP). By adjusting the pattern parameters in the size of the tested bacterial strain *E. coli* K12 WT(BW25113) to allow for increased bacteria/surface contact area, bacterial viability could be significantly reduced in comparison to smooth reference surfaces. In addition, aging-related alteration of wettability of the patterned surfaces allowed for detailed investigation of the combined influences of molecular surface condition and contact favoring topography on the antimicrobial properties of Cu. The presented results form a suitable basis for the targeted optimization of copper-based antimicrobial contact surfaces by surface functionalization using ultrashort pulsed laser irradiation.

2. Results

2.1. Surface Characterization

The morphology as well as the topographic parameters of surface patterns induced by USP-DLIP on metals have been previously shown to be tailorable by adjusting the fluence in respect to the individual thermal substrate interaction.[43] Here, an
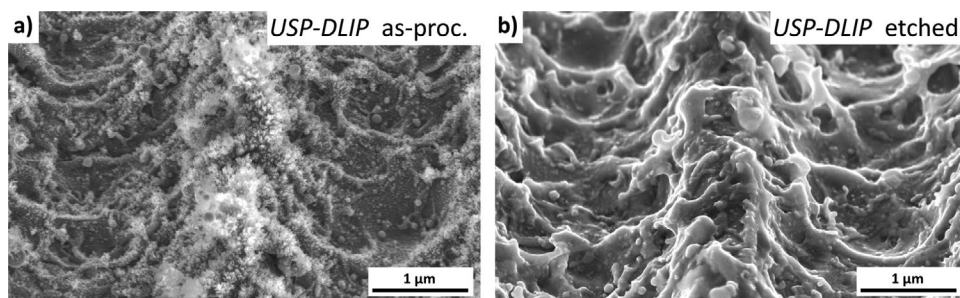
Figure 1. SEM images of pattern peaks on USP-DLIP-processed Cu surfaces representing the individual topographies before and after post-treatment by immersion etching. a) Cu surface processed by 3 J cm^{-2} in as-processed state; b) Cu surface processed by 3 J cm^{-2} after immersion etching using 3 % citric acid.

alteration of the occurring ablation mechanisms by increasing the applied laser fluence has to be considered as well, since it prominently affects both primary pattern and sub-structure parameters. In the case of Cu, ablation behavior changes between spallation and phase explosion, as soon as substrate heating surpasses the threshold temperature of $T_{PE} = 0.9 \times T_{cr}$ with a critical temperature T_{cr} of 7696 K,[44] which is shown to affect both peak geometry as well as surface morphology.[43] To create line pattern geometries befitting the scale of single cells of the tested *E. coli* K12 strain, laser parameters were adjusted to a fluence of 3 J cm^{-2} and pattern periodicity of 3 µm, which lead to ablation in the phase explosion regime on the utilized oxygen free Cu (OF-Cu) material.[43] The resulting surface morphologies both in as-processed as well as post-treated state are illustrated in **Figure 1**.

The USP-DLIP patterns exhibit narrow peaks framed by spatially expanded valleys where material ablation during processing took place. The ratio of the total surface area distributed between the two topographic features corresponds ≈29%/71% (peaks/valleys). In the as-processed state, these surfaces contain flake-like nanostructures, which concentrate mainly on the peak regions, as visible in Figure 1a. In a former study, these sub-structures could be identified as agglomerations of Cu$_2$O formed by re-deposition of ablated matter during USP-DLIP processing.[45] Post-processing by immersion etching in 3% citric acid was shown to fully remove surface oxide revealing both the metallic substrate material as well as a surface morphology mainly induced by mobilized and rapidly cooled melt fronts resulting from the phase explosion ablation mechanism

(see Figure 1b). Consequently, the surface roughness Rq is highest in the peak area of the as-processed surfaces, which can be attributed to the flake-like sub-structure, since in case of the immersion etched samples peak roughness almost equals the roughness measured in the valleys, as presented in **Table 1**. In contrast to the peak regions, roughness in the valley areas shows no alteration before and after chemical post-processing.
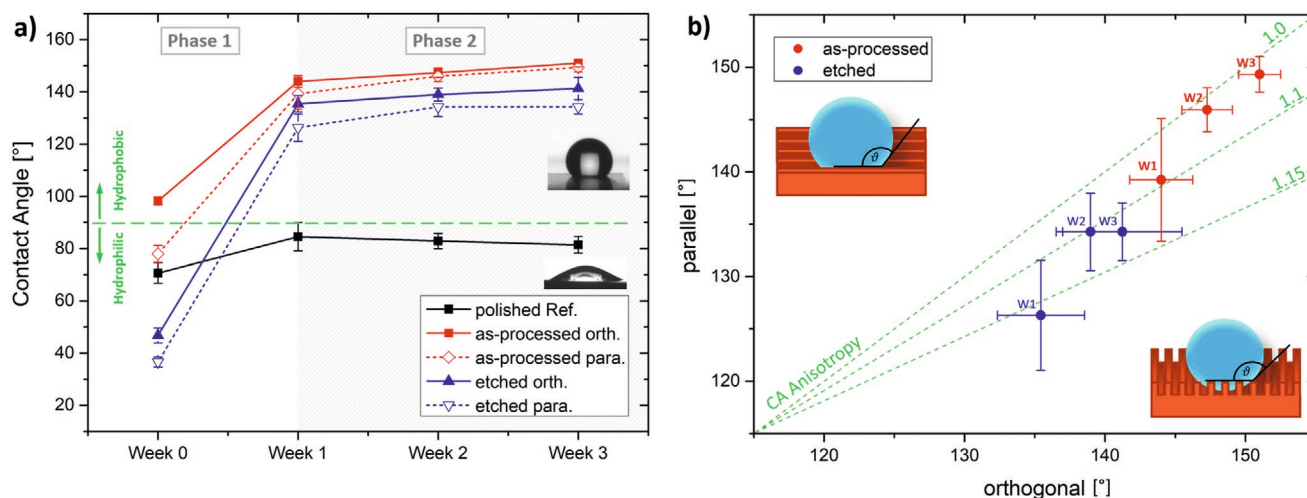
In USP-DLIP processing, pattern depth was set to 1 µm, which leads to an increase of surface area by factor 1.6 (*S*-value) in comparison to the flat surface topography of polished Cu samples. Minor alteration of the *S*-value in between as-processed and etched surfaces can be attributed to surface roughening induced by the oxidic sub-structures.

2.2. Wettability

The wetting behavior of the different Cu surfaces was measured in relation to the duration of storage in ambient environment starting from 24 h after processing (Week 0) and repeating the measurement every 7 days on a yet unused sample. Wetting behavior of all patterned samples followed a similar trend of rapidly enhancing hydrophobicity during aging within the first week starting from low contact angles (CA) that is followed by leveling at slightly higher CA within 2 more weeks of aging as visible in **Figure 2**. This effect has been reported for Cu surfaces processed by ultrashort pulsed laser irradiation before and can be traced back to a prominent agglomeration of functional carbon groups of C-C/C-H bonding type,[46,47] which

Table 1. Surface parameters of USP-DLIP patterns applied on Cu surfaces in the as-processed and immersion etched state.

	USP-DLIP as-proc.	USP-DLIP etched
Valley width [µm]	2.19 $^{+/- 0.12}$	
Depth [µm]	1.055 $^{+/- 0.084}$	1.016 $^{+/- 0.058}$
Rq peak [nm]	188.5 $^{+/- 30.5}$	97.3 $^{+/- 28.3}$
Rq valley [nm]	90.3 $^{+/- 12.3}$	94.2 $^{+/- 12.2}$
S-value	1.61	1.57

**ADVANCED
SCIENCE NEWS**

www.advancedsciencenews.com

**ADVANCED
MATERIALS
INTERFACES**

www.advmatinterfaces.de

Figure 2. Modification of surface wetting behavior on Cu samples processed by USP-DLIP in relation to aging under ambient atmosphere: a) Aging-related alteration of CA in orthogonal and parallel orientation to the line-like pattern also highlighting the two different phases of either rapid CA increase or CA leveling; b) development of droplet shape anisotropy during atmospheric aging in Phase 2.

was also recently verified for the surfaces investigated in this study.[45] However, the rapid increase in CA has to be emphasized especially for as-processed USP-DLIP surfaces where elevated values around 90° could be detected already 24 h after laser processing (see Figure 2a,b).

The quick attainment of high CA values in the first aging phase indicates a prominent effect of sticking on the droplet spreading by the rough surface topography alongside the chemical modification during aging, which also leads to higher drop shape anisotropy as spreading is less suppressed parallel to the line pattern orientation (compare Figures 2a and 2b). Besides the minor overall CA increase, the second aging phase highlighted in Figure 2a is characterized by further approximation of the CA values measured in orthogonal and parallel orientation of the line patterns leading to reduced drop shape anisotropy. As soon as this approximation reaches a stable level, falling droplets would bounce off the patterned surfaces in horizontal alignment, while they tend to stick on the surface before. This change indicates a transition between Wenzel and Cassie–Baxter like wetting of the surfaces, where sufficient sticking by penetration of the pattern grooves is no longer possible. This assumption is supported by measured values of advancing and receding contact angles that are less than 15° in case of the non-sticking surfaces, while on sticking surfaces they are significantly higher. On as-processed surfaces, this state is reached already after 2 weeks, while 3 weeks of aging are needed in case of immersion etched samples.

The higher CA reached for as-processed surfaces (illustrated in Figure 2a), as well as the low droplet shape anisotropy stabilized already after the second week of aging (see Figure 2b) appear to be linked to the roughness values R_q measured on the peak areas of the different surfaces, indicating an enhancing effect of the process-induced flake-like sub-structure on hydrophobic wetting behavior. A similar increase of CA was also observed on micrometer patterns by Allahyari et al.,[48] which was traced back to a more pronounced nanoparticle decoration of the surfaces during processing with higher laser fluence. It

has to be noted that the ratio of agglomeration between hydrophilic carbo-oxygen and hydrophobic C-C/C-H bonding species was shown to vary in favor of the latter type on as-processed surfaces during aging in a recent study, while a similar ratio was already stabilized after 24 h of aging on immersion etched samples.[45] Hence, wetting of as-processed surfaces would be expected to show a more pronounced hydrophilic behavior in comparison to etched surfaces slightly after processing from a chemical aspect. However, CA measurements show the opposite, which highlights the significant influence of the difference in surface roughness.
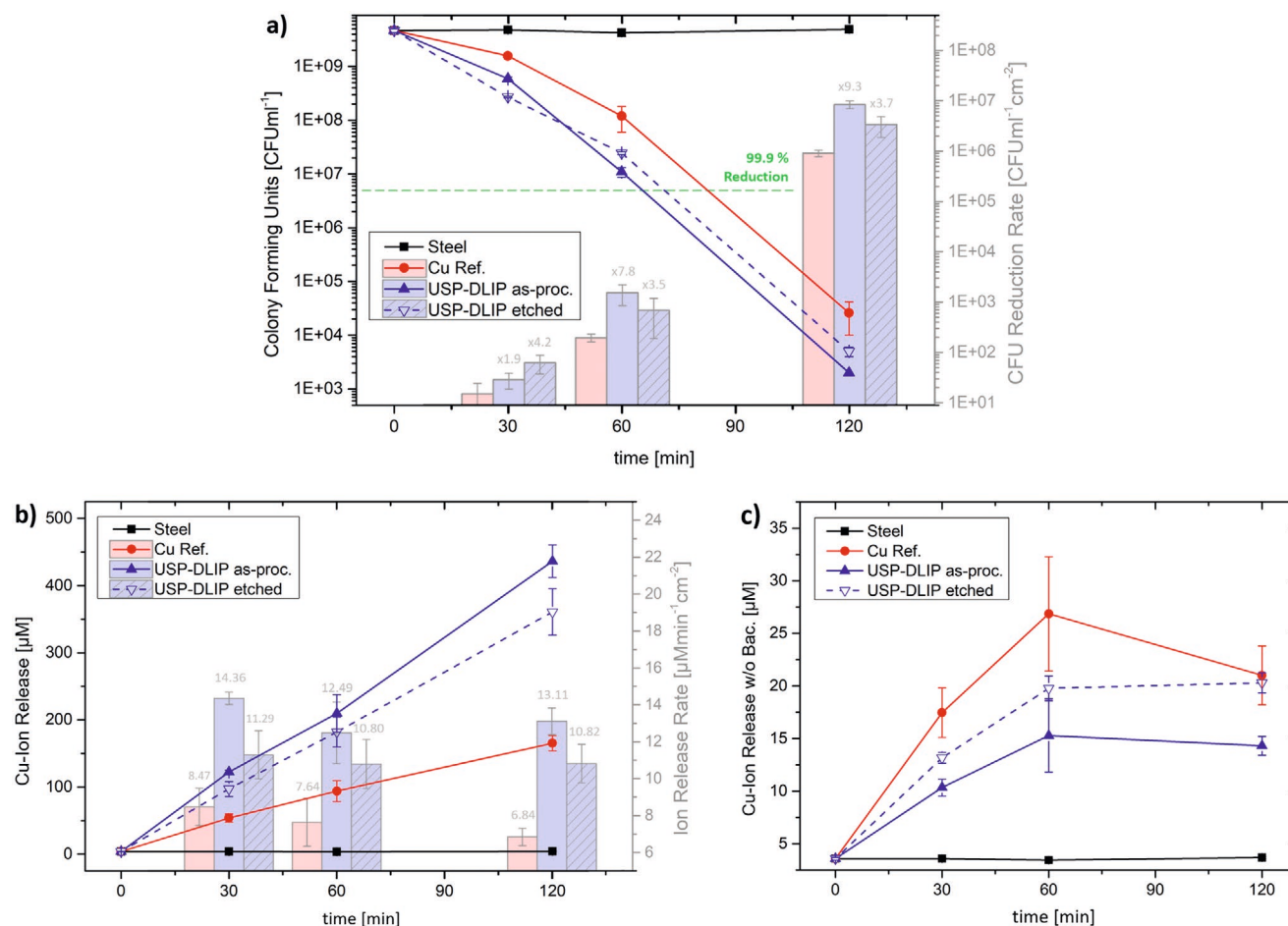
2.3. Antibacterial Properties

2.3.1. Antibacterial Effect of USP-DLIP Processing

The previous results show a prominent impact of the process-related flake-like sub-structure on topographical and wetting properties of USP-DLIP Cu surfaces. To involve the influence of the oxidic sub-structure on antibacterial properties in the investigation of the actual impact of topographic patterning in the scale range of single bacteria cells, wet plating tests were conducted on both as-processed and immersion etched USP-DLIP Cu surfaces. Testing was conducted after 3 weeks of aging of each the USP-DLIP as well as the polished reference surfaces, by which the patterned samples showed distinctive (super-)hydrophobic wetting, while the references were slightly hydrophilic (Figure 2a). A uniform droplet/metal contact area on all samples was achieved by applying the wet plating methodology involving hydrophobic adhesive tape rings described in more detail in Experimental Section.

The results of the wet plating tests illustrated in **Figure 3**a show a considerable reduction of viable bacteria detectable on the different tested Cu surfaces with increasing exposure time. Although the polished Cu reference already shows high antibacterial efficiency against the tested *E. coli* strain, the USP-DLIP surfaces patterned in the scale range of single bacteria

**ADVANCED
SCIENCE NEWS**

www.advancedsciencenews.com

**ADVANCED
MATERIALS
INTERFACES**

www.advmatinterfaces.de

Figure 3. Illustrations showing the results of wet plating tests on USP-DLIP surfaces after 3 weeks of aging: a) CFU reduction of *E. coli* on the different Cu surfaces in relation to an inert steel reference. CFU values normalized to actual surface area show an increase of up to 9.3-fold of USP-DLIP surfaces against polished Cu. b) Cu ion release measured on the individual surfaces alongside CFU reduction. c) Cu Ion release in case of PBS application without bacteria.

cells exceed these values both in the case of as-processed and immersion etched state. While on polished Cu, viable cell count reduction reaches a critical amount of 99.9%[13] after ≈85 min, the same level is reached on the USP-DLIP surfaces already between 60 and 70 min. Surprisingly, the antibacterial properties of as-processed surfaces seem to exceed those of immersion etched samples after 60 min despite a significantly higher amount of surface oxidation,[14,45] whereas the post-treated surfaces dominate in bacterial killing in the first 30 min. Comparison of the colony forming units (CFUs) reduction rate in relation to the smooth Cu reference reveal a 4.5-fold enhancement on immersion etched surfaces in this early phase, which decreases to ≈3.6-fold during further exposure. On as-processed surfaces, this trend is reversed as CFU reduction rate continuously increases up to 9.3-fold of the values measured on the Cu reference after 120 min exposure while starting at 1.9-fold in the first phase.

Parallel examination of the Cu ion release during the experiment, as displayed in Figure 3b, reveals a considerable increase of Cu emission in comparison to the Cu reference on both USP-DLIP surfaces. Despite the presence of a dense oxide layer, ion release of the as-processed surfaces exhibits the

highest values, which appears to be the reason for the high CFU reduction observed. Here, the dominance of Cu_2O in the chemical composition of the oxidic sub-structure[45] seems to induce an overall positive effect on the antibacterial properties, as it shows minor reduction of Cu ion release in relation to pure Cu.[14] In combination with the increased surface/area ratio of the flake-like sub-structure expressed by the Rq values presented in Table 1, the overall balance appears to be in favor of an additional enhancement of Cu emission and hence antibacterial efficiency on as-processed in comparison to immersion etched USP-DLIP surfaces. The thin superficial layer of CuO that was determined on both surfaces via XPS depth profiling does not appear to affect Cu ion release, here.[45] In addition to the overall increase of Cu emission, the ion release rate of both USP-DLIP surfaces remain on a stable high level after a peak during the first 30 min of exposure, while on the Cu reference ion release rate continuously drops throughout the whole experiment as presented in Figure 3b. It must be emphasized that the discussed CFU reduction rate as well as the Cu ion release rate are directly related to the real surface and include the surface enlargement on USP-DLIP surfaces by involving the S-value. The actual enhancement of CFU reduction determined

**ADVANCED
SCIENCE NEWS**
www.advancedsciencenews.com

**ADVANCED
MATERIALS
INTERFACES**
www.advmatinterfaces.de

on immersion etched and as-processed USP-DLIP Cu surfaces in relation to the smooth reference accounts to 6- and 15-fold. Therefore, the observed enhancement of these two properties cannot be attributed to the increase in surface area caused by laser structuring but seems to be related to a beneficial bacteria/surface interaction, instead.

Analyzation of Cu ion release under exposure to PBS without bacteria on the other hand reveals a comparably low Cu emission on all surfaces, as displayed in Figure 3c: Both polished Cu and immersion etched USP-DLIP surfaces reach almost equal emission values after 120 min of exposure, which might be traced back to a similar surface chemistry mainly consisting of a native oxide layer leading to analogous passivation behavior. However, the etched USP-DLIP surfaces show a more leveled gradient of Cu emission also visible in case of the as-processed surfaces, which indicates a slightly different passivation process of the laser processed samples. Cu ion release on as-processed USP-DLIP surfaces stagnates at a considerably lower level related to a higher passivating effect of the process-related Cu_2O layer. Here, the high surface/area ratio of the flake-like oxide topography does not appear to increase Cu ion release in contrast to the behavior observed in the presence of bacteria.

Bacteria have been recently reported to affect Cu ion release during wet plate testing using PBS as they act as drains for Cu ions, which prevents chemical surface passivation by oxide formation and leads to the maintenance of a constantly high corrosion-induced ion emission rate.[13] Against this background, USP-DLIP surface modification appears to additionally enhance this effect leading to a significant increase in Cu ion release in the presence of bacteria compared to flat Cu surfaces, while corrosion resistance is actually enhanced after laser treatment, as indicated by the reduced emission values without bacteria. This especially accounts for as-processed samples exhibiting the highest difference of Cu ion release with and without bacteria as well as the highest killing efficiency.

It has been reported before that dead cells are accumulating more copper in the cytosol than living cells, where membrane damage might induce the increased uptake of copper ions from the medium due to concentration gradients.[41,49] Furthermore, dead cells cannot discard the copper ions via efflux pumps which might also be a factor for increased Cu accumulation inside dead bacterial cells. Thereby it has to be questioned if the increase in antibacterial efficiency and Cu ion release on as-processed surfaces might be affected by additional mechanical damaging of the bacteria by the flake-like oxidic sub-structure, like, for example, on *Cicada* and *Dragonfly* wing surfaces[32,33] and short pulsed laser treated Cu surfaces.[38,39] In order to investigate this more closely, scanning electron microscopy (SEM) imaging of formaldehyde-fixated bacteria after wet plating was conducted to get a hint on the dominant mode of action in bacteria killing on as-processed USP-DLIP surfaces. Since formaldehyde has a low pH value, bacteria fixation is accompanied by intense corrosive attack of the Cu surfaces, especially visible in the peak areas of USP-DLIP patterns, whereby this statement must be made primarily by observing the morphology of adhering bacteria.

The distribution of the bacteria over the surface area shows a clear preference of the valleys for adhesion, as displayed in **Figure 4**a, where peak regions appear to be mainly occupied by greater clusters expanding out of neighboring valleys. Bacteria morphology in the valleys shows no change compared to conspecifics adhering to flat reference surfaces (see Figure 4c), while single bacteria cells attached to peak areas often exhibit a shortened cell body, in contrast. No indication of topography-induced membrane damage is visible on most of the imaged bacteria cells aside of individual specimen that appeared to be collapsed due to leaking (see Figure 4b). However, relating to the low level of visible cell damage which can be observed likewise on polished reference surfaces as visible in Figure 4c, membrane damage is more likely to be caused by interaction with Cu ions, here.[9]

In the light of these investigations, the major mode of action leading to increased antibacterial efficiency of the USP-DLIP surfaces appears to be an amplification of Cu ion induced toxic stress. It was shown that bacteria have mechanisms for sensing if they are attached to a surface which include cell appendages (flagella, pili, curli) or envelope deformations resulting in envelope stress.[50] After sensing the surface attachment, phenotypic changes from the planktonic life form toward a sessile state appear to be initiated, where metabolism alters to now focus on the formation of biofilms.[50] Compared to previous results, these phenotypic changes in relation to surface contact might influence the uptake of ions such as copper ions and hence the efficiency of copper mediated killing, even though the exact mechanisms are not completely understood yet.[12,51]

2.3.2. Influence of Wetting Behavior on Antibacterial Efficiency

The significant enhancement of the antibacterial properties of Cu surfaces by USP-DLIP processing, in parts also despite increased surface oxidation, indicates a pristine bacteria/surface interaction on the laser-induced topographies. In case of ultrashort pulsed laser processing, chemical surface modification also involves an aging related change in wettability, which is also observed here (see Figure 2). As surface wettability is shown to have a huge effect on bacterial adhesion,[22,25] possible changes of bacteria/surface interaction might also lead to an alteration of the antibacterial efficiency of USP-DLIP surfaces. To further investigate this, wet plating tests were conducted on as-processed and immersion etched USP-DLIP samples after 24 h and 3 weeks of aging under ambient atmosphere. With reference to the results presented in Figure 2a, the different aging periods lead to either hydrophilic wetting after 24 h or (super-) hydrophobic wetting after 3 weeks.

Bacterial viability of the tested *E. coli* K12 strain on both Cu reference and the USP-DLIP surfaces aged for 3 weeks show a similar relation like in the previous experiment, exhibiting a predominant antibacterial efficiency of the laser-treated samples with increased bacterial killing rates on as-processed samples after 60 and 120 min exposure (see **Figure 5**a). CFU reduction on USP-DLIP samples after 24 h of aging show a comparable relation between as-processed and immersion etched samples after 120 min, although bacterial viability appears to be less decreased here. However, the etched surfaces of the hydrophilic samples remain more efficient in bacterial killing even after
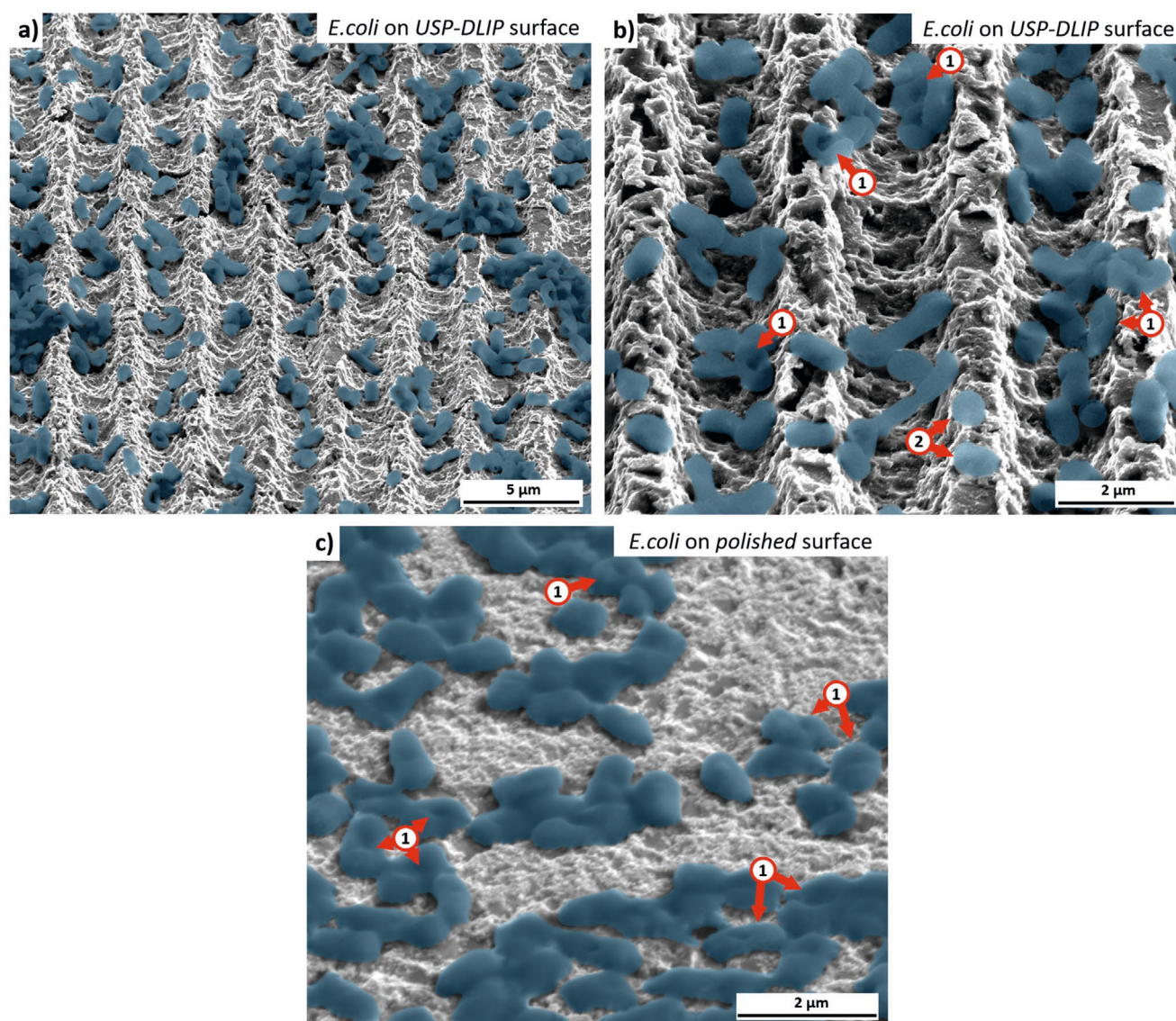
Figure 4. SEM images of *E. coli* (blue) on as-processed USP-DLIP and polished Cu surfaces fixated by 4% formaldehyde. a) Overview showing single bacteria cells and clusters. b) Close-up revealing several collapsed cells (1). Bacteria in peak areas show a more shortened morphology (2) compared to bacteria in valley regions. c) Bacteria on polished Cu surfaces showing similar collapsing (1) compared to cells on USP-DLIP surfaces. The visible surface roughening is due to corrosive attack during fixation after the wet plating experiment and not related to bacteria/surface interaction.

60 min of exposure compared to as-processed surfaces despite significantly lower Cu ion release (compare Figure 5b). In addition, CFU reduction in relation to surface area falls below the values of the copper reference in the first two measuring points on both hydrophilic USP-DLIP surfaces. The slightly decreased overall bacterial viability after 120 min of exposure might be linked rather to increased Cu ion release instead of favorable bacteria/surface interaction, here.

By directly comparing hydrophobic and hydrophilic USP-DLIP samples, a clearly lower antibacterial efficiency can be determined for the hydrophilic laser treated surfaces, although Cu ion release does not deviate noteworthy from the values measured on the hydrophobic surfaces, as displayed in Figure 5b. The almost identical course of the Cu emission on etched samples both after 24 h and after 3 weeks of aging is particularly striking when related to the significantly different CFU reductions measured in parallel. A similar trend can be observed between the different as-processed USP-DLIP surfaces, whereas it must be emphasized that bacterial killing on the hydrophilic as-processed samples still falls below the values of etched hydrophobic samples after 120 min despite significantly higher Cu ion release. This illuminates the grave influence of surface chemistry on the bacteria/surface interaction, which in turn has a significant effect on the antimicrobial effectiveness of Cu surfaces. It appears that both increased Cu ion release and bacteria/surface contact area in case of the as-processed surfaces only lead to an improved efficiency in bacterial killing, if bacteria are facing wetting properties that might be preferential for adhesion. The same relation accounts to immersion etched samples, whereas it has to be noted that Cu
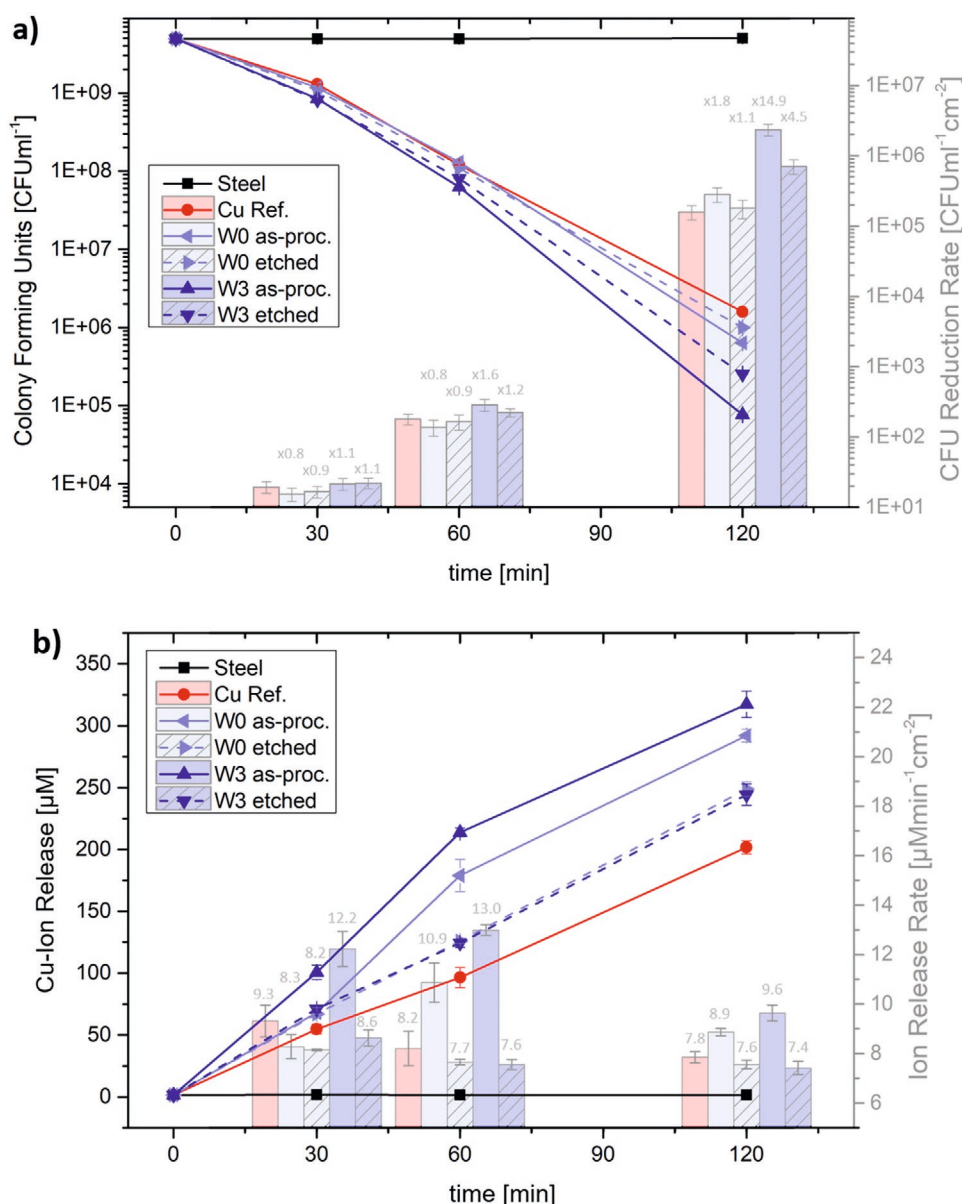
Figure 5. Results of the wet plating tests in correlation to surface wetting properties: a) Reduction of detectable CFU count of *E. coli* K12 during wet plating tests on either hydrophilic (W0) or (super-)hydrophobic (W3) USP-DLIP surfaces in relation to a smooth Cu reference; b) Cu ion release on the different tested surfaces measured alongside CFU reduction.

ion release rate in relation to surface area of both hydrophobic and hydrophilic surfaces run lower than the values of the Cu reference in this experiment. However, the lower ion emission does not appear to affect antibacterial efficiency of the two different surfaces as much as the differences in wetting properties, where hydrophobic etched samples again exhibit increased bacterial killing, even despite low ion release, while the antimicrobial properties of the hydrophilic sample approximate the Cu reference when related to the relative surface.

From these results, the hydrophilic etched samples actually appear to reflect the antibacterial properties of the Cu reference surface transmitted to an increased ratio of surface area, while hydrophobic wetting induces bacteria/surface interaction on the very same surface topography that enhances the antibacterial effect of Cu even without an actual increase of Cu ion release, in contrast. In case of as-processed USP-DLIP surfaces, increased bacteria killing rates in comparison to etched surfaces are linked to a prominently enhanced Cu ion release rate, which however still needs to be coupled with preferential wetting properties to reach its full potential in bacteria killing.

It has to be noted here that bacteria killing as well as Cu ion release showed an overall decrease compared to the previous experiment as visible by comparing Figures 3 and 5, where especially a lower relative CFU reduction on hydrophobic USP-DLIP samples after 60 min of exposure as well as lower Cu ion release on both of the etched surfaces stand out. The underlying reason might be aging of the bacterial culture

**ADVANCED
SCIENCE NEWS**

www.advancedsciencenews.com

**ADVANCED
MATERIALS
INTERFACES**

www.advmatinterfaces.de

during storage at 4 °C for 2 months between both experiments leading to a reduced metabolic activity of the bacteria. Warnes and Keevil showed that the DNA of dead cells denatures much more slowly on Cu surfaces, suggesting that metabolic activity is involved in the expression of the initial superoxide-mediated killing.[52] By this, a significant antibacterial effect on Cu surfaces might be delayed in case of reduced metabolic activity.

2.3.3. Bacterial Attachment during Surface Wetting

Aside of the significantly increased Cu ion release, as-processed USP-DLIP surfaces exhibit a characteristic lag phase, where bacterial killing remains below the values of etched samples despite higher Cu ion release. In the case of hydrophobic samples, this phase includes the first sampling time after 30 min, while it seems to still continue after 60 min for hydrophilic samples (compare Figures 3a and 5a). A possible reason for this behavior might be reduced bacteria/surface interaction, for example, by reduced adhesion during the initial contact phase due to the increased nano-scale roughness of surfaces exhibiting the flake-like sub-structure.[28] To investigate bacterial mobility and adhesion alongside propagating surface wetting on the different tested surfaces in situ investigations were conducted by means of confocal laser scanning microscopy (LSM). The specified setup used in the investigation, where the wetting front propagation of PBS with and without bacteria between the tilted sample surface and a glass substrate is imaged, is described in detail in the experimental section. To facilitate a detection of bacteria and their activity in LSM, a strain of *E. coli* (ClearColi BL21(DE3)) expressing green fluorescent protein (GFP) and exhibiting similar properties as *E. coli* K12 WT(BW25113) was utilized. Propagation of the wetting front was recorded in situ by imaging the reflection signal of wetted partitions of the sample surface, while the location of bacteria in relation to the surface and wetting front was recorded through alternating imaging of the fluorescence signal (see **Figure 6**a). In order to determine the surface-specific wetting behavior in relation to the various topographical surface characteristics with parallel inclusion of a possible bacterial influence, the drop spreading velocity of PBS with and without bacteria was measured in parallel orientation of the line patterns. The presented results focus on USP-DLIP samples after 3 weeks of aging as well as the Cu reference, since the pronounced hydrophilic wetting behavior of samples aged for 24 h leads to elevated drop expansion speeds too high to perform imaging of the drop front. Videos of the drop edge propagation alongside bacterial attachment on the different surfaces referring to the images shown in Figure 6 are provided in Supporting Information.

The main influence on bacterial mobility turned out to be sedimentation, through which the majority of bacteria are detected on or in close proximity to the glass substrate below the sample surfaces after 20 min without additional fluid dynamics involved. The additional drag induced by capillary forces in the utilized testing method on the other hand leads to fluid currents by which the planktonic bacteria gets flushed between the sample surface and glass substrate. Most of the bacteria still continue sedimentation, whereas individual cells or clusters in the vicinity of the sample surfaces might adhere

in case the attractive surface forces surpass both fluid drag and gravity force.

In case of the smooth topography of the polished Cu reference samples, the propagation speed of the drop edge was too fast to allow for continuous switching between the two signal channels, whereas imaging was either focusing one or the other signal, as illustrated in Figure 6a. Records of the droplet propagation reveal a straight wetting front spreading at a speed of either 10.41 µms^{-1} without and 11.38 µms^{-1} with bacteria. Imaging the fluorescence signal emitted by the bacteria shows a slightly increased density of bacteria along the wetting front, which are getting pushed over the surface without adhering, while bacteria from the subsequent medium flow manage to adhere instead. The adhering units appear to mainly be composed of clusters instead of single cells, especially in closer vicinity to the wetting front pointing out that fluid drag in this area represents a major obstacle to the adhesion of bacteria. However, attractive forces appear to induce interaction between the bacteria and the surface enabling adhesion as soon as fluid drag gets reduced. From the data received, the bacteria approach to the Cu surface appears to be mainly due to currents in the media, while self-motion capability of individual cells might additionally contribute to the final contacting in close vicinity to the substrate.

On USP-DLIP surfaces, imaging using the reflection contrast shows the pattern valleys as bright lines separated by dark areas attributed to the peak regions where surface inclination significantly weakens the signal (illustrated in Figure 6b). In case of immersion etched USP-DLIP surfaces, the wetting front exhibits a slightly less straight progression along the pattern compared to the Cu reference both with and without bacteria. Wetting propagation speed is significantly reduced to ≈159.59 nms^{-1} without and 877.22 nms^{-1} with bacteria that marks out both a decreasing effect of the hydrophobic surface properties on wetting propagation as well as a significant alteration of surface wetting in the presence of bacteria on this type of surface. Adhesion of bacteria mainly takes place in the vicinity of the droplet edge, which is most likely linked to a lower fluid drag due to the lower wetting propagation speed in comparison to the Cu reference. Adhering bacteria occupy both peak and valley regions but are detected more frequently in the valleys (see Figure 6b) indicating a positive effect of concave topography features on bacteria/surface interaction.

Droplet propagation on as-processed samples is significantly reduced compared to both the Cu reference as well as immersion etched samples. Imaging of surfaces exposed to PBS without bacteria exhibits a weak reflection signal alongside a distorted course of the wetting front along the surface pattern. The propagation speed of the drop edge runs at a very slow level of ≈51.61 nms^{-1} until droplet intrusion is finally stopped by pinning of the wetting front a few tens of micrometer after the sample edge, where the water-repellent forces of the hydrophobic surface seem to come into equilibrium with the counteracting forces induced by the measurement setup. As soon as bacteria are present in the medium, droplet propagation is slightly increased to a speed of ≈61.39 nms^{-1} also showing a continuous wetting front expansion although localized pinning is still apparent, as visible in Figure 6c. Planktonic bacteria detected in the medium appear solely in the wetting front
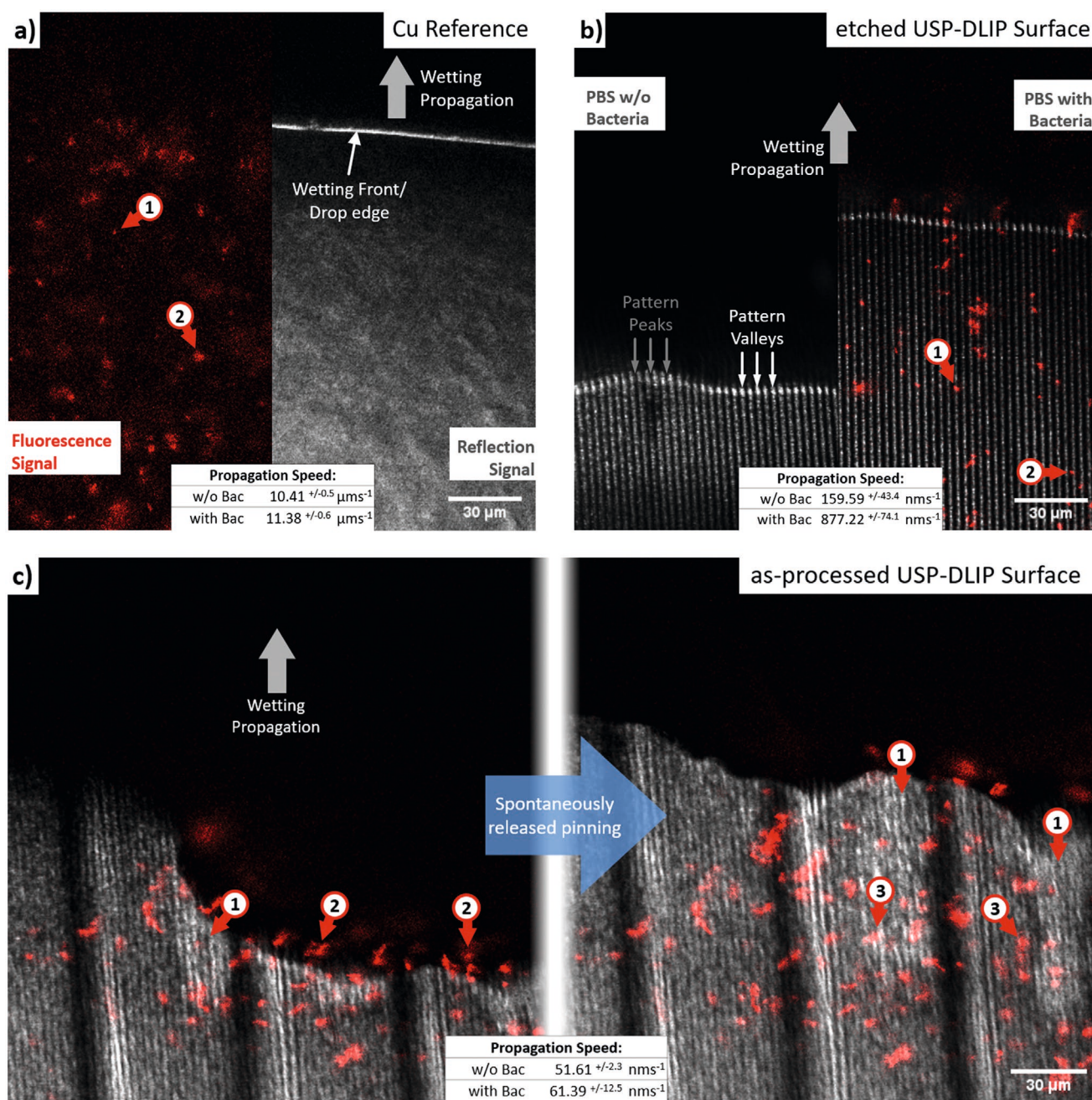
Figure 6. Imaging of the wetting propagation on the different Cu samples: a) wetting front propagation on a smooth Cu reference surface imaged parallel to bacterial attachment by LSM using fluorescent *E. coli* separated in reflection signal showing the substrate surface, as well as the fluorescent signal showing single cells (1) and clusters of bacteria (2). b) Wetting of an immersion-etched USP-DLIP surface by PBS with and without bacteria. Adhering bacteria are found in the valley (1) as well as the peak areas (2). c) Wetting on as-processed USP-DLIP surface showing areas of altered wetting state (1) alongside local pinning and release events related to adhesion of bacteria (3) that were previously floating close to the drop edge (2).

pointing out a rather low fluid drag, but a predominant influence of propagation induced currents near the drop interface on bacteria dispersed within the droplet volume close to the substrate surface. Bacteria leaving the droplet edge directly attach to the substrate surface, where they are fully immobilized leading to adhesion observed solely along the wetting front. In case of single bacteria cells and smaller clusters, attached bacteria are predominantly located within the pattern valleys, while larger clusters also manage to cover peak areas. However, initial attachment points of these clusters are also located within the valley regions indicating preferential bacterial adhesion in these areas, which might be attributed to the difference in nano-scaled surface roughness Rq in between the two areas.[28] These observations correspond very well with the distribution of the bacteria visible in Figure 4a,b. It has to be emphasized that in several events a spontaneous release of localized pinning could

**ADVANCED
SCIENCE NEWS**

www.advancedsciencenews.com

**ADVANCED
MATERIALS
INTERFACES**

www.advmatinterfaces.de

be observed in relation to the presence of bacteria close to the drop edge, which appeared to contribute to further propagation of surface wetting (displayed in Figure 6c). Here, attractive forces between patterned surface and bacteria seem to form an additional antipole to the hydrophobic properties, which shifts the balance of forces at the wetting front in favor of a progressive wetting. Alongside these events, changes in the reflection contrast of the valley areas point out localized changes of the wetting state.

Considering these observations in the in situ LSM investigations, a clear influence of specific surface features on bacterial adhesion and surface wetting on the different examined surfaces can be determined:

On as-processed USP-DLIP surfaces, wetting involving bacteria is expressed less by an increase in wetting propagation speed but moreover by the destabilization of localized droplet pinning. Wetting without bacteria appears to stabilize in a Cassie–Baxter state, where the pattern valleys are not penetrated by the liquid and contribute to a pinning of the drop edge. Once bacteria are involved, this state gets destabilized allowing both medium as well as bacteria to enter the valleys, which also reduces the previously observed pinning in the peak areas. Bacteria are predominantly attached to valley regions pointing out a low suitability of the peak regions for adhesion, whereas bacterial attachment can be assumed to be locally suppressed until full surface wetting is achieved. In fact, previous literature has already pointed out the repelling effect of surface topographies exhibiting feature sizes smaller than the scale of single bacteria cells.[28,31] These results complement the SEM observations discussed earlier which are illustrated in Figure 4.

On immersion etched surfaces, instead, wetting observed via LSM appears to exhibit a low stability of a Cassie–Baxter and rather the appearance of a Wenzel state, which is further enhanced in the presence of bacteria. These examinations fit to the late change between sticking and bounce off behavior during wetting tests involving falling droplets after 3 weeks of atmospheric aging, as discussed earlier. In contrast to the as-processed surfaces, bacteria attach to pattern peaks more often showing a higher suitability for adhesion of these regions after post-processing.

In that regard, the deviation of the overall wetting behavior and bacterial adhesion between the two types of USP-DLIP samples appears to be mainly contributable to the filigree morphology of the flake-like sub-structure found on the peaks of as-processed surfaces effecting reduced wettability[48] and bacterial adhesion[28] due to increased nano-scale roughness. Alongside the preliminary Cassie–Baxter wetting state, especially the suppressed adhesion of bacteria on the rough surface peaks in the early state of surface wetting on as-processed USP-DLIP surfaces appear to be the reason for the lower bacterial killing rates measured after 30 min in the wet plating experiments in relation to immersion etched surfaces even despite higher Cu ion release rates. This illustrates the necessity of a direct and pronounced contact between bacteria and Cu surface, as already postulated by Mathews et al.[12] to enable a strong expression of antibacterial properties. In this context, the reduced bacterial killing on hydrophilic USP-DLIP surfaces, as displayed in Figure 5a, might be attributed to lower adhesion forces between bacteria and the surface, similar to the results of Maikranz

et al.[22]. This is particularly evident in the prolonged lag phase of hydrophilic as-processed samples, where increased surface roughness and reduced adhesion forces between bacteria and surface appear to negatively interact. However, the exact mechanism of bacterial adhesion alongside altered sensitivity against Cu ions has to be clarified more precisely. Contrary to the *S. aureus* used in ref. [22], *E. coli* has a significantly lower hydrophobicity of the cell surfaces, which might be reflected in a weaker surface adhesion.[53] Therefore, preceding protein attachment preferring hydrophobic surfaces could also play a role here.[54]

3. Conclusion

We were able to show that surface functionalization via USP-DLIP treatment has a significant effect on the antibacterial properties of Cu surfaces. The results allow for a better understanding of the role of bacteria/surface interaction in the expressed Cu sensitivity of bacteria as well as an improved design of contact surfaces to enhance antibacterial properties of copper surfaces:

- Reduction of viable cell count of *E. coli* on Cu surfaces in wet conditions is enhanced by USP-DLIP patterning in the scale range of single bacteria cells leading to a relative increase of up to ≈ 6-fold in case of post-processed and 15-fold in case of as-processed surfaces. The enhancement of killing efficiency surpasses the capacities of sole enlargement of available surface area indicating a beneficial effect on bacteria/surface interaction, which induces higher sensitivity of the bacteria against Cu intoxication.

- Cu ion release is increased in the presence of bacteria, which especially accounts for USP-DLIP surfaces in as-processed condition. In contrast, Cu emission falls below the smooth Cu reference in exposure to PBS without bacteria. Hence, increased Cu ion release can be directly connected to bacterial Cu draining which was previously reported,[13] however with a much stronger effect on the laser structured surfaces. As-processed USP-DLIP surfaces exhibit the greatest differences in Cu ion release indicating an opposite corrosion behavior of the oxidic flake-like substructure with and without bacteria.

- Although increased Cu ion release exhibits a beneficial influence on antibacterial efficiency, the reduction of viable cell count appears to be influenced to a larger extent through quality and quantity of contact to the surface. This predominantly involves surface wettability, where hydrophilic USP-DLIP surfaces exhibit significantly lower effectiveness against *E. coli* compared to hydrophobic USP-DLIP surfaces, even despite higher Cu ion release.

- Furthermore, reduced bacterial attachment on the peaks of the as-processed samples was observed compared to immersion etched samples, indicating a repelling effect of the nanoscale substructure.[28] Together with a lower bacterial contact in the initial phase of the wet plating experiments, reduced bacterial killing on these surfaces can be observed despite high Cu ion emission. This effect is particularly noticeable on the hydrophilic sample, which further illustrates the strong influence of

topographic and chemical surface properties on the antibacterial effectiveness of Cu surfaces.

The presented results show the possibilities of targeted surface functionalization to increase the antibacterial effectiveness of Cu contact surfaces to the same extent as they illustrate the necessity of a precise knowledge of the dominant influencing factors in order to achieve a maximum increase in efficiency. By this, they allow for a more targeted approach to the design of copper-based antibacterial surfaces that increases their effectivity beyond the toxic effect of emitted Cu ions itself.

4. Experimental Section

Sample Preparation: Sheets of OF-CU (>99.95%) (Wieland) and AISI 304 stainless steel (Brio) of the dimensions 10×25 mm^2 were mirror-polished on an automated TegraPol-21 system (Struers). Shares of the polished Cu samples as well as the steel samples were deducted for their later use as references in the wet plating experiments.

The remaining Cu samples were laser processed by USP-DLIP utilizing a Ti:Sapphire Spitfire laser system (Spectra Physics) emitting a pulse duration of t_p = 100 fs (full width at half maximum) at a centered wavelength λ of 800 nm and 1 kHz pulse frequency. Two beam laser interference was achieved by using the optical setup previously introduced in ref. [43] consisting of a diffractive optical element to divide and a lens system to overlap the individual beams on the sample surfaces. The periodicity p of the generated pattern in correlation to the incident angle θ can be calculated by Equation (1) utilizing the analogy of the beam paths in the interference setup to the setup of the Fresnel mirror test:

$$p = \frac{\lambda}{2 \tan(\theta)} \tag{1}$$

Planar patterning was conducted in continuous pulsing mode at a fluence of 3 J cm^{-2} and 90% pulse overlap. The periodicity of the applied patterns was set to 3 μm, by which the achieved topography closely fits the bacterial size of the tested *E. coli* K12 strain. A batch of samples was subsequently selected to undergo immersion etching in 3% citric acid for 40 s in an ultrasonic bath to remove process-induced oxidic substructures on the pattern surfaces.[45]

Wetting Tests: CA measurements were conducted to examine aging-related alterations of surface wettability of the different sample surfaces by means of a Drop Shape Analysator DSA 100 (Krüss GmbH) using distilled water at a fixed droplet volume of 3 μL. Due to the anisotropic surface patterns, the CA was detected in orthogonal and parallel orientation to the pattern on the USP-DLIP samples. In a parallel experiment, falling droplet tests are conducted by releasing the droplets at a height of 100 mm above horizontally aligned USP-DLIP treated surfaces leading to either sticking or bouncing off.

For the investigation of wetting front propagation and bacterial adhesion LSM experiments were performed on an inverted Zeiss LSM 880 with a 40× Fluar N.A 1.30 oil immersion objective. The patterned (or smooth for reference) Cu sample was held upside down in a glass-bottom dish by means of a sticking 300 μm thick spacer. The topography of the surface was imaged in reflection mode using a 20% reflection/80% transmission beam splitter and the detection of bacteria was achieved in the 530 nm range of the emitted light (emission of GFP). For both signal, 488 nm laser light was used as excitation.

The fluorescent bacteria are derived from the *E. coli* strain ClearColi BL21(DE3) from Lucigen. The strain was transduced with a pBAD-sfGFP plasmid in order to produce super-folder Green Fluorescent GFP (sfGFP) in the presence of arabinose. For each experiment, cells were freshly thawed 24 h, and arabinose was added 2 h before image acquisition. Short before imaging, the bacteria were diluted in PBS similar to the wet plating tests. A drop of 500 μL of the solution was deposited in close proximity of the metal sample and image acquisition was started immediately with a frequency of one image per 3 s. Capillary forces as well as fluid pressure would lead to a penetration of the solution into the narrow space between sample and glass surface due to hydrophilic wetting properties of the glass substrate exhibiting a CA of 62°. The experimental setup is schematically illustrated in **Figure 7**.
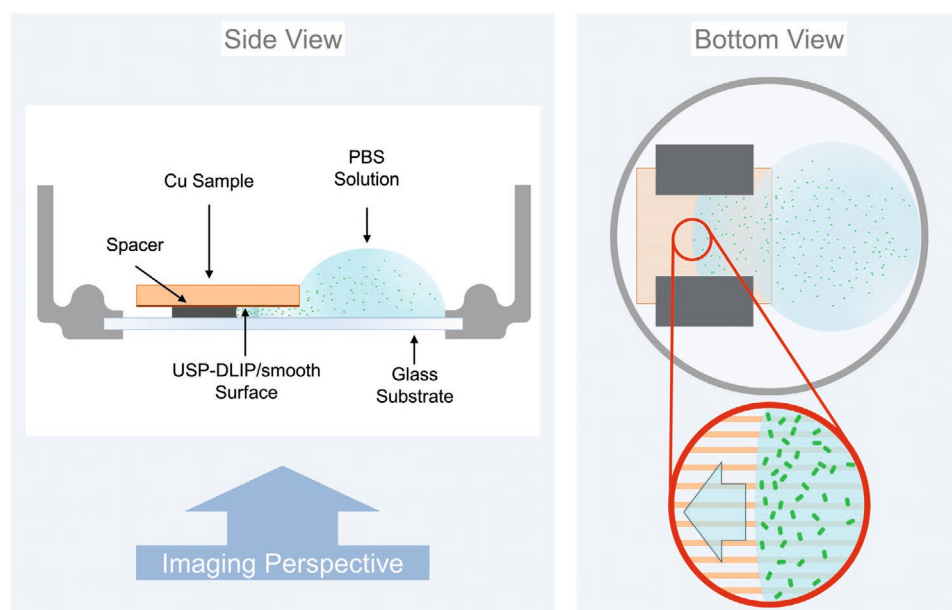
Figure 7. Schematic illustration of the experimental setup used to investigate wetting propagation on the smooth and USP-DLIP-processed Cu surfaces. Cu samples are mounted upside down to allow for imaging in the inverse LSM forming a cavity of 300 μm spacing with the glass substrate of the sample holder below. Droplets of PBS solution with and without bacteria that are applied aside of the copper sample penetrate the cavity with a wetting front speed related to the wettability of the sample surface.
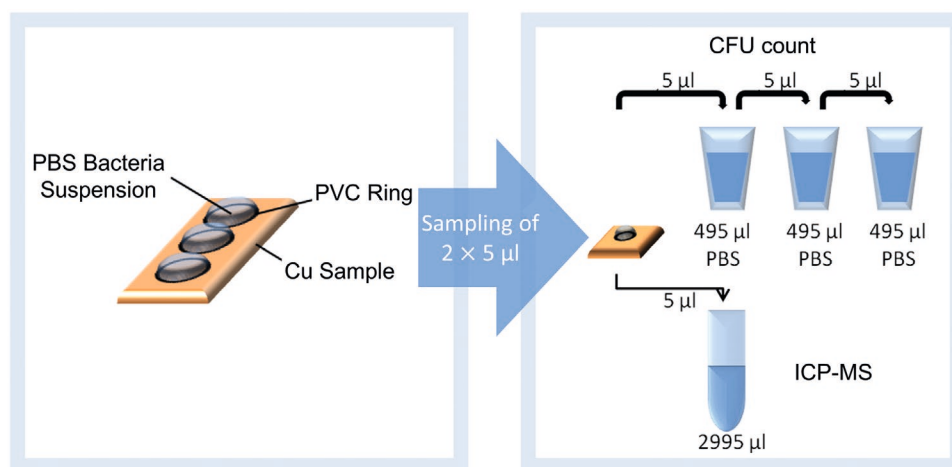
Figure 8. Schematic illustration of the wet plate testing setup used in the experiments involving surfaces of different wetting properties utilizing rings of polyvinyl chloride (PVC) adhesive tape to predefine the exposed surface area. Both colony forming units (CFU) and Cu ion released are measured in parallel.

Antibacterial Properties: *E. coli* K12 WT(BW25113) was cultured following the protocol of Molteni et al.[55] by aerobic overnight growth in Lysogeny broth (LB) medium at 37 °C with a shaking speed of 220 rpm. The stationary cells were collected from 5 mL culture medium by centrifugation for 15 min at $5000 \times g$, followed by three consecutive PBS washing steps involving the same centrifugation parameters. The final bacteria testing solution (BTS) was gained by resuspension in 5 mL of PBS. The initial average cell count following this routine ranges from 3×10^9–5×10^9 CFU mL^{-1}. Bacteria of the *E. coli* K12 WT(BW25113) strain were provided on Agar plates by the group of Prof. Rolf Müller from the Helmholtz Centre of Infection Research, Saarbrücken and stored at 4 °C.

Following the wet plating method, three droplets of 40 µL of the BTS were applied on each sample stored in water saturated environment from which two doses of each 5 µL were withdrawn after individual exposure intervals (30 min, 60 min, and 120 min). Resuspension of settled bacteria was conducted by vigorous pipetting where a parallel orientation of the tip to the surface pattern avoids shadowing of the bacteria attached in the pattern valleys. The cell count of bacteria was determined via the standard plate count method, whereby one of the 5 µL doses was serially diluted in PBS and spread on LB agar plates, which were incubated at 37 °C and 80% moisture overnight to enable counting of the remaining CFUs after the individual exposure intervals. The second 5 µL dose was diluted 600-fold in 0.1% HNO₃ and used to determine the corresponding Cu ion concentrations in the BTS by inductively coupled plasma mass spectrometry (Agilent 7500cx).

The wet plating experiments aimed to compare the antibacterial properties of USP-DLIP patterned samples to polished flat Cu surfaces, as well as patterned samples with different surface characteristics involving both topography and chemistry. To allow for comparability in between samples of different wetting properties, a novel wet plating routine was developed where the contact area between BTS and the sample surface was predefined by rings of polyvinyl chloride (PVC) adhesive tape exhibiting an inner diameter of 5 mm. Due to their hydrophobic wetting behavior, the PVC rings prevent the droplets from further expansion in case of hydrophilic sample surfaces, while they can be used to expand the droplet over the whole area inside the rings in case of (super-) hydrophobic surfaces using the adhesive tape as anchorage for the edges of the droplets, as schematically illustrated in **Figure 8**.

Surface Characterization: Characterization of the topographical properties of the differently processed USP-DLIP Cu samples was conducted by means of both confocal laser scanning microscopy (CLSM) utilizing a LEXT OLS4100 3D Measuring Laser Microscope by Olympus and SEM (Helios 600 by FEI). The CLSM measurements were done utilizing the 50× lens and altering the digital post-magnification between 2× and 6× at a laser wavelength of 405 nm and focusing the

detection of topographic surface parameters including, for example, roughness and surface/projected area ratio (S-value). SEM imaging was conducted in secondary electron (SE) contrast mode while the samples were tilted 52° degree to allow for better visualization of topographical features. The acceleration voltage was set to either 10 or 5 kV at a current of 0.86 pA. To allow investigation of bacterial cell morphology alongside the detection of preferential contacting areas on the surface, samples that underwent wet plating for 60 min were immersed in 4% formaldehyde for 12 h to assure stabilization of the cell shape in vacuum followed by immersion in sterilized distilled water for another 10 min to wash off remnants from PBS.

Supporting Information

Supporting Information is available from the Wiley Online Library or from the author.

Conflict of Interest

The authors declare no conflict of interest.

[1] L.-Y. Sobisch, K. M. Rogowski, J. Fuchs, W. Schmieder, A. Vaishampayan, P. Oles, N. Novikova, E. Grohmann, *Front. Microbiol.* **2019**, *10*, 543.

[2] E. P. Lesho, M. Laguio-Vila, *Mayo Clin. Proc.* **2019**, *94*, 1040.

[3] M. Colin, E. Charpentier, F. Klingelschmitt, C. Bontemps, C. De Champs, F. Reffuveille, S. C. Gangloff, *J. Hosp. Infect.* **2020**, *104*, 283.

[4] E. A. Bryce, B. Velapatino, H. A. Khorami, T. Donnelly-Pierce, T. Wong, R. Dixon, E. Asselin, *Biointerphases* **2020**, *15*, 011005.

[5] J. J. Hostýnek, H. I. Maibach, *Copper and the Skin*, Informa Healthcare, New York **2006**.

[6] S. Krupanidhi, A. Sreekumar, C. B. Sanjeevi, *Indian J. Med. Res.* **2008**, *128*, 448.

[7] S. Kim, J. E. Choi, J. Choi, K. H. Chung, K. Park, J. Yi, D. Y. Ryu, *Toxicol. In Vitro* **2009**, *23*, 1076.

[8] M. Croes, S. Bakhshandeh, I. A. J. van Hengel, K. Lietaert, K. P. M. van Kessel, B. Pouran, B. C. H. van der Wal, H. C. Vogely, W. Van Hecke, A. C. Fluit, C. H. E. Boel, J. Alblas, A. A. Zadpoor, H. Weinans, S. A. Yavari, *Acta Biomater.* **2018**, *81*, 315.

[9] G. Grass, C. Rensing, M. Solioz, *Appl. Environ. Microbiol.* **2011**, *77*, 1541.

[10] M. Hans, S. Mathews, F. Mücklich, M. Solioz, *Biointerphases* **2016**, *11*, 018902.

[11] N. van Doremalen, T. Bushmaker, D. H. Morris, M. G. Holbrook, A. Gamble, B. N. Williamson, A. Tamin, J. L. Harcourt, N. J. Thornburg, S. I. Gerber, J. O. Lloyd-Smith, E. de Wit, V. J. Munster, *N. Engl. J. Med.* **2020**, *382*, 1564.

[12] S. Mathews, M. Hans, F. Mücklich, M. Solioz, *Appl. Environ. Microbiol.* **2013**, *79*, 2605.

[13] J. Luo, C. Hein, J. Ghanbaja, J. Pierson, F. Mücklich, *Micron* **2019**, *127*, 102759.

[14] M. Hans, A. Erbe, S. Mathews, Y. Chen, M. Solioz, F. Mücklich, *Langmuir* **2013**, *29*, 16160.

[15] C. Sun, Y. Li, Z. Li, Q. Su, Y. Wang, X. Liu, *J. Nanomater.* **2018**, *2018*, 6546193.

[16] J. Al-Haddad, F. Alzaabi, P. Pal, K. Rambabu, F. Banat, *Clean Technol. Environ. Policy* **2020**, *22*, 269.

[17] A. Ananth, S. Dharaneedharan, M. S. Heo, Y. S. Mok, *Chem. Eng. J.* **2015**, *262*, 179.

[18] A. Tripathy, A. Kumar, S. Sreedharan, G. Muralidharan, A. Pramanik, D. Nandi, P. Sen, *ACS Biomater. Sci. Eng.* **2018**, *4*, 2213.

[19] E. Ozkan, C. C. Crick, A. Taylor, E. Allan, I. P. Parkin, *Chem. Sci.* **2016**, *7*, 5126.

[20] M. Polívková, T. Hubáček, M. Staszek, V. Švorčík, J. Siegel, *Int. J. Mol. Sci.* **2017**, *18*, 419.

[21] C. A. P. Bastos, N. Faria, J. Wills, P. Malmberg, N. Scheers, P. Rees, J. J. Powell, *NanoImpact* **2020**, *17*, 100192.

[22] E. Maikranz, C. Spengler, N. Thewes, A. Thewes, F. Nolle, P. Jung, M. Bischoff, L. Santen, K. Jacobs, *Nanoscale* **2020**, *12*, 19267.

[23] M. C. M. van Loosdrecht, W. Norde, J. Lyklema, A. J. B. Zehnder, *Aquat. Sci.* **1990**, *52*, 103.

[24] J. H. Pringle, M. Fletcher, *Appl. Environ. Microbiol.* **1983**, *45*, 811.

[25] A. H. A. Lutey, L. Gemini, L. Romoli, G. Lazzini, F. Fuso, M. Faucon, R. Kling, *Sci. Rep.* **2018**, *8*, 10112.

[26] C. Díaz, M. C. Cortizo, P. L. Schilardi, S. S. G. G. de, M. M. A. F. L. de, *Mater. Res.* **2007**, *10*, 11.

[27] A. K. Epstein, A. I. Hochbaum, P. Kim, J. Aizenberg, *Nanotechnology* **2011**, *22*, 494007.

[28] R. Helbig, D. Günther, J. Friedrichs, F. Rößler, A. Lasagni, C. Werner, *Biomater. Sci.* **2016**, *4*, 1074.

[29] D. Guenther, J. Valle, S. Burgui, C. Gil, C. Solano, A. Toledo-Arana, R. Helbig, C. Werner, I. Lasa, A. F. Lasagni, in *SPIE 9736, Laser-based Micro- and Nanoprocessing X*, SPIE, Bellingham, WA **2016**.

[30] K. Schwibbert, F. Menzel, N. Epperlein, J. Bonse, J. Krüger, *Materials* **2019**, *12*, 3107.

[31] A. Peter, A. H. A. Lutey, S. Faas, L. Romoli, V. Onuseit, T. Graf, *Opt. Laser Technol.* **2020**, *123*, 105954.

[32] A. Tripathy, P. Sen, B. Su, W. H. Briscoe, *Adv. Colloid Interface Sci.* **2017**, *248*, 85.

[33] A. Elbourne, R. J. Crawford, E. P. Ivanova, *J. Colloid Interface Sci.* **2017**, *508*, 603.

[34] S. Ghosh, S. Niu, M. Yankova, M. Mecklenburg, S. M. King, J. Ravichandran, R. K. Kalia, A. Nakano, P. Vashishta, P. Setlow, *Sci. Rep.* **2017**, *7*, 17768.

[35] T. Sjöström, A. H. Nobbs, B. Su, *Mater. Lett.* **2016**, *167*, 22.

[36] J. V. Wandiyanto, T. Tamanna, D. P. Linklater, V. K. Truong, M. Al Kobaisi, V. A. Baulin, S. Joudkazis, H. Thissen, R. J. Crawford, E. P. Ivanova, *J. Colloid Interface Sci.* **2020**, *560*, 572.

[37] J. Hasan, H. K. Webb, V. K. Truong, S. Pogodin, V. A. Baulin, G. S. Watson, J. A. Watson, R. J. Crawford, E. P. Ivanova, *Appl. Microbiol. Biotechnol.* **2013**, *97*, 9257.

[38] L. B. Boinovich, V. V. Kaminsky, A. G. Domantovsky, K. A. Emelyanenko, A. V. Aleshkin, E. R. Zulkarneev, I. A. Kiseleva, A. M. Emelyanenko, *Langmuir* **2019**, *35*, 2832.

[39] V. Selvamani, A. Zareei, A. Elkashif, M. K. Maruthamuthu, S. Chittiboyina, D. Delisi, Z. Li, L. Cai, V. G. Pol, M. N. Seleem, R. Rahimi, *Adv. Mater. Interfaces* **2020**, *7*, 1901890.

[40] A. M. Emelyanenko, V. V. Kaminskii, I. S. Pytskii, A. G. Domantovsky, K. A. Emelyanenko, A. V. Aleshkin, L. B. Boinovich, *Bull. Exp. Biol. Med.* **2020**, *168*, 488.

[41] A. M. Emelyanenko, I. S. Pytskii, V. V. Kaminsky, E. V. Chulkova, A. G. Domantovsky, K. A. Emelyanenko, V. D. Sobolev, A. V. Aleshkin, L. B. Boinovich, *Colloids Surf., B* **2020**, *185*, 110622.

[42] L. B. Boinovich, K. A. Emelyanenko, A. G. Domantovsky, E. V. Chulkova, A. A. Shiryaev, A. M. Emelyanenko, *Adv. Mater. Interfaces* **2018**, *5*, 1801099.

[43] D. W. Müller, T. Fox, P. G. Grützmacher, S. Suarez, F. Mücklich, *Sci. Rep.* **2020**, *10*, 3647.

[44] S. Y. Wang, Y. Ren, C. W. Cheng, J. K. Chen, D. Y. Tzou, *Appl. Surf. Sci.* **2013**, *265*, 302.

[45] D. W. Müller, A. Holtsch, S. Lößlein, C. Pauly, C. Spengler, S. Grandthyll, K. Jacobs, F. Mücklich, F. Müller, *Langmuir* **2020**, *36*, 13415.

[46] A. M. Kietzig, M. N. Mirvakili, S. Kamal, P. Englezos, S. G. Hatzikiriakos, *J. Adhes. Sci. Technol.* **2011**, *25*, 2789.

[47] J. Long, M. Zhong, P. Fan, D. Gong, H. Zhang, *J. Laser Appl.* **2015**, *27*, S29107.

[48] E. Allahyari, J. J. J. Nivas, S. L. Oscurato, M. Salvatore, G. Ausanio, A. Vecchione, R. Fittipaldi, P. Maddalena, R. Bruzzese, S. Amoruso, *Appl. Surf. Sci.* **2019**, *470*, 817.

[49] M. Köller, N. Ziegler, C. Sengstock, T. A. Schildhauer, A. Ludwig, *Biomed. Phys. Eng. Express* **2018**, *4*, 055002.

[50] T. E. P. Kimkes, M. Heinemann, *FEMS Microbiol. Rev.* **2020**, *44*, 106.

[51] R. Nandakumar, C. E. Santo, N. Madayiputhiya, G. Grass, *BioMetals* **2011**, *24*, 429.

[52] S. L. Warnes, C. W. Keevil, *Appl. Environ. Microbiol.* **2011**, *77*, 6049.

[53] V. Kochkodan, S. Tsarenko, N. Potapchenko, V. Kosinova, V. Goncharuk, *Desalination* **2008**, *220*, 380.

[54] G. B. Sigal, M. Mrksich, G. M. Whitesides, *J. Am. Chem. Soc.* **1998**, *120*, 3464.

[55] C. Molteni, H. K. Abicht, M. Solioz, *Appl. Environ. Microbiol.* **2010**, *76*, 4099.